ELSEVIER

Journal of Organometallic Chemistry 569 (1998) 225–233

Journal of Organometallic Chemistry

Face-to-face fixed ferrocenes. Synthesis and properties of 2,10-diferrocenyl- and 2,5,7,10-tetraferrocenyl-1,6-methano[10]annulenes

Masahiko Iyoda [a,*], Toshitaka Okabe [a], Motomi Katada [b], Yoshiyuki Kuwatani [a]

[a] *Department of Chemistry, Graduate School of Science, Tokyo Metropolitan University, Hachioji, Tokyo 192-0397, Japan*
[b] *Radioisotope Research Center, Tokyo Metropolitan University, Hachioji, Tokyo 192-0397, Japan*

Received 3 June 1998

Abstract

2,10-Diferrocenyl- and 2,5,7,10-tetraferrocenyl-1,6-methano[10]annulenes, in which the ferrocene nuclei are held proximate and cofacial, have been synthesized by using the palladium-catalyzed cross-coupling reaction of ferrocenylzinc chloride with 2,10-dibromo- and 2,5,7,10-tetrabromo-1,6-methano[10]annulenes. The structures of the face-to-face fixed ferrocene systems were determined by X-ray analysis. Cyclic voltammetric measurements of diferrocenyl- and tetraferrocenyl-1,6-methano[10]annulenes show two and three redox waves, respectively, reflecting the through-space and through-bond interactions of the ferrocene nuclei.

Keywords: 1,6-Methano[10]annulenes; Palladium-catalyzed cross-coupling; Electron donors; Ferrocenes; Redox properties

1. Introduction

The face-to-face fixed metallocene system (**1**) has received considerable attention from both theoretical and experimental chemists [1,2], because the two metallocene moieties in this system may reveal either through-space or through-bond interaction in the neutral (**1**), mono-cation (**2**), and dication states (**3**) [3–6], and because polymeric mixed-valence metallocene systems can be expected to show either ferromagnetic properties based on **4** or interesting columnar organometallic structures (**5** and **6**). On the basis of these expectations, we studied the synthesis and properties of diferrocenyl- and tetraferrocenyl-1,6-methano[10]annulenes (**7**, **8** and **9**) (Fig. 4).

2. Results and discussion

2.1. Synthesis

Recently, we developed a new synthetic method of di-, tri- and tetraferrocenylarenes using a transition-metal-catalyzed coupling reaction [7]. We applied this convenient method for the synthesis of di- and tetraferrocenyl-1,6-methano[10]annulenes (**7**, **8** and **9**). As shown in Scheme 1, the reaction of ferrocene (**10**) in THF with *t*-butyllithium (1.34 equivalents) at 0°C for 30 min, followed by treatment with $ZnCl_2$ at 0°C to room temperature produced ferrocenylzinc chloride (**11**) in a good yield. The cross-coupling reaction of 2,10-dibromo-1,6-methano[10]annulene (**12**) [8] with **11** (3 equivalents) in the presence of $PdCl_2(PPh_3)_2$ (10 mol%) in THF at room temperature for 1 h proceeded smoothly to give 2,10-diferrocenyl-1,6-methano[10]-annulene (**7**) in 49% yield. In a similar manner, the reaction of 2,7-dibromo-1,6-methano[10]annulene (**13**)

* Corresponding author. Fax: +81 426 772525.

0022-328X/98/$ - see front matter
PII S0022-328X(98)00791-8

[9] with **11** (3 equivalents) in the presence of $PdCl_2(PPh_3)_2$ (10 mol%) in THF produced the corresponding cross-coupling product (**8**) in 47% yield. Interestingly, this palladium-catalyzed cross-coupling reaction can be satisfactorily applied to the synthesis of 2,5,7,10-tetraferrocenyl-1,6-methano[10]-annulene (**9**). Thus, the reaction of 2,5,7,10-tetrabromo-1,6-methano[10]annulene (**14**) [10] with **11** (6 equivalents) in the presence of $PdCl_2(PPh_3)_2$ (20 mol%) in THF produced **9** in 29% yield. Although a similar palladium-catalyzed cross-coupling of dihalogenoarenes with **11** (3 equivalents) afforded the corresponding diferrocenylarenes in 60–80% yields, the yields of **7**–**9** were decreased to 47–49%, presumably due to the steric hindrance between the peri-substituents at the second coupling reaction. 2,5,7,10-Tetrasubstituted annulene (**9**) was obtained in a reasonable yield by considering the twofold steric effect between the peri-substituents.

2.2. Structures and properties

2.2.1. X-Ray analysis

In order to gain insight into the structures of 2,10-diferrocenyl- and 2,5,7,10-tetraferrocenyl-1,6-methano[10]annulenes (**7** and **9**), single crystal X-ray analyses were carried out. Fig. 1 and Fig. 2 show ORTEP representations, while Table 1, Table 2and Table 3 give relevant structural data. As shown in Fig. 1, two cyclopentadienyl rings attached to the annulene ring are fixed face-to-face and are rotated about 40° from the least-squares plane of the annulene ring which is comparable to the value (average 46°) of similar distortion in 1,8-diferrocenylnaphthalene (**15**) ([2]a). Although the two cyclopentadiene rings in **7** cause severe steric strain on the annulene ring, the intramolecular C(1)···C(6) distance is 2.29 Å, slightly longer than the corresponding 2.235 Å found in the parent 1,6-methano[10]annulene (**16**) [11], i.e. the annulene part has an aromatic 10 π-electronic character. The steric strain in this molecule is relieved by using the bending and distortion between the C(2)–C(12) and C(10)–C(22) bonds. Thus, the intramolecular C(12)···C(22) distance, which reflects the bending of these bonds, is 3.19 Å, much longer than the corresponding 2.96 Å found in **15**, although the C(2)···C(10) distance (2.57Å) is similar to the corresponding C(1)···C(8) distance (2.56Å) in **15**. As shown in Fig. 1b, the two ferrocene parts attached to the annulene ring indicate a distortion of the C(2)–C(12) and C(10)–C(12) bonds, and the dihedral angle between these bonds is 28° which relieves the steric repulsion between the ferrocene moieties and the annulene ring in **7** (Fig. 5).

As shown in Fig. 2a, **9** has a crystallographic mirror plane through the central bridge carbon atom C(6) and the midpoints of the C(1)–C(1*) and C(5)–C(5*) bonds. Although **9** can be expected to suffer a large steric strain like 1,4,5,8-tetraphenylnaphthalene (**17**) [12], which suffers considerable strain than that of 1,8-diphenylnaphthalene (**18**) [13], the central annulene ring retains a symmetrical structure. The C(1)···C(6) distance in **9** is 2.27 Å, indicating the cycloheptatriene structure of the annulene ring. The two pairs of substituted cyclopentadienyl rings are positioned face-to-face and rotated about 57° from the least-squares plane of the annulene ring. In a similar manner as **7** and 2,5,7,10-tetrakis(trimethylsilyl)-1,6-methano[10]-annulene (**19**) [14], the steric strain in **9** is relieved

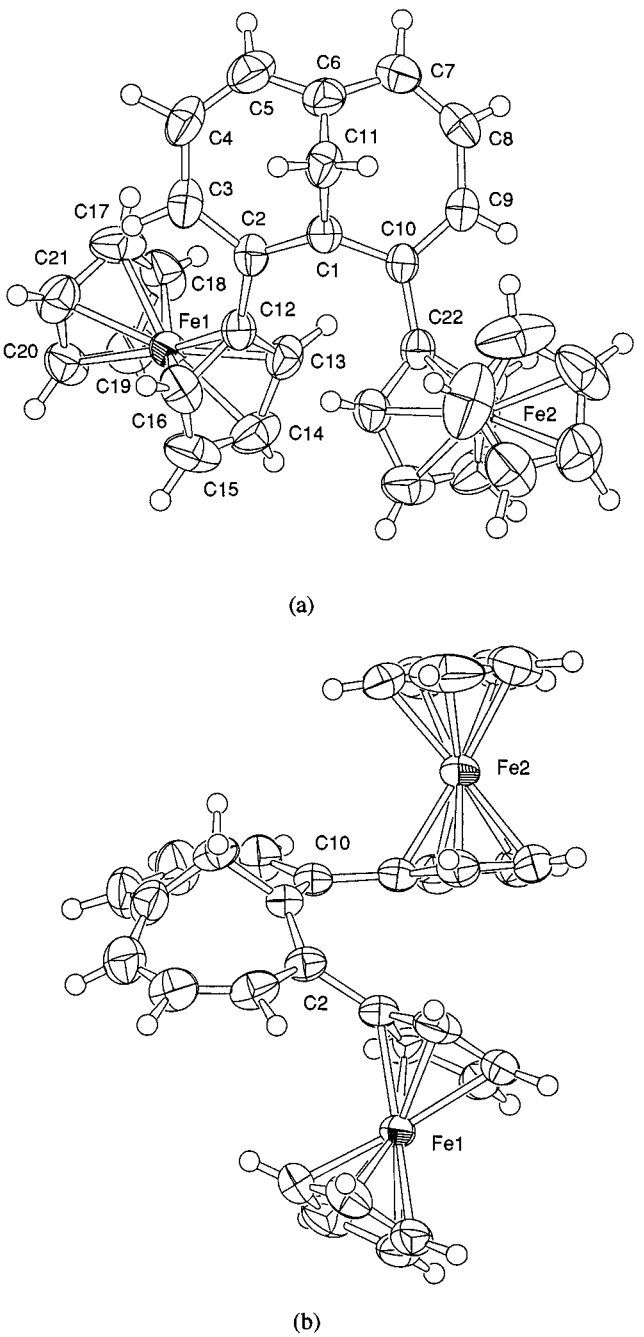

Fig. 1. The molecular structure of **7**. (a) Top view. (b) Side view.

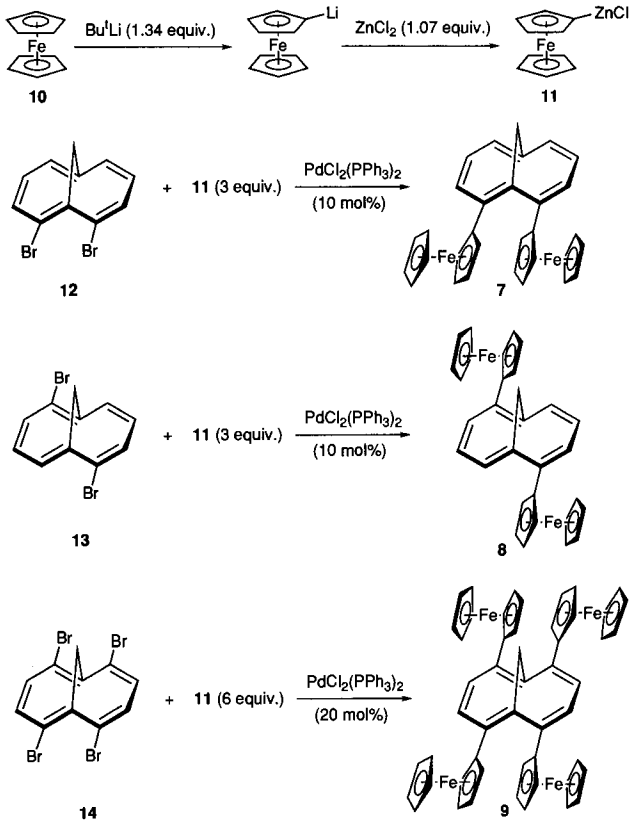

Scheme 1.

by the bending and distortion between the C(2)–C(7) and C(4)–C(17) bonds. Interestingly, the intramolecular C(2)···C(4) distance is 3.09 Å, slightly shorter than that of **7**, and the dihedral angle between C(2)–C(7) and C(4)–C(17) is 20° in **9**, slightly smaller than that of **7**. Thus, the more severely strained molecule **9** shows a smaller distortion of the four ferrocene moieties as compared with **7**. This conflict can be resolved by considering the flexibility of the 1,6-methano[10]-annulene system and the rotation of the cyclopentadienyl rings. The steric strain in **9** is mainly relieved by deformation of the annulene ring, i.e. the elongation of the C(2)–C(3) and C(3)–C(4) bonds [1.43(2) Å] and the spread of the C(2)–C(3)–C(4) angle [128(1)°]. In addition, the cyclopentadienyl rings in **9** (ca. 57°) are rotated much more than in **7** (ca. 40°) from the least-squares plane of the annulene ring, which diminishes the strain energy.

2.2.2. Spectroscopic studies

The ^{1}H-NMR spectra of di- and tetraferrocenyl-1,6-methano[10]annulenes (**7**–**9**) give interesting structural information in solution (Table 4). 1,6-Methano[10]annulene is known to possess a stable 10 π-electron system, and the inner bridge protons shift remarkably to upper field (δ −0.5) and the outer olefinic protons shift to lower field (δ 6.8–7.5) [15]. On the other hand, ferrocene (**10**) is one of the most stable organometallic compounds, and its cyclopentadienyl ring shows a 6 π-aromatic character. Therefore, **7** and **9** can be regarded as a crowded biaryl system like 1,8-diphenyl and 1,4,5,8-tetraphenylnaphthalenes (**18** and **17**). As is distinct from a mobile phenyl group in **17** and **18** [16], however, the ^{1}H-NMR spectra of **7**–**9** were temperature-independent, and all protons in **7**–**9** were observed as a simple first-order pattern (Fig. 6).

The ^{1}H-NMR spectra of **7**–**9** show five ferrocene protons, i.e. one singlet of unsubstituted cyclopentadi-

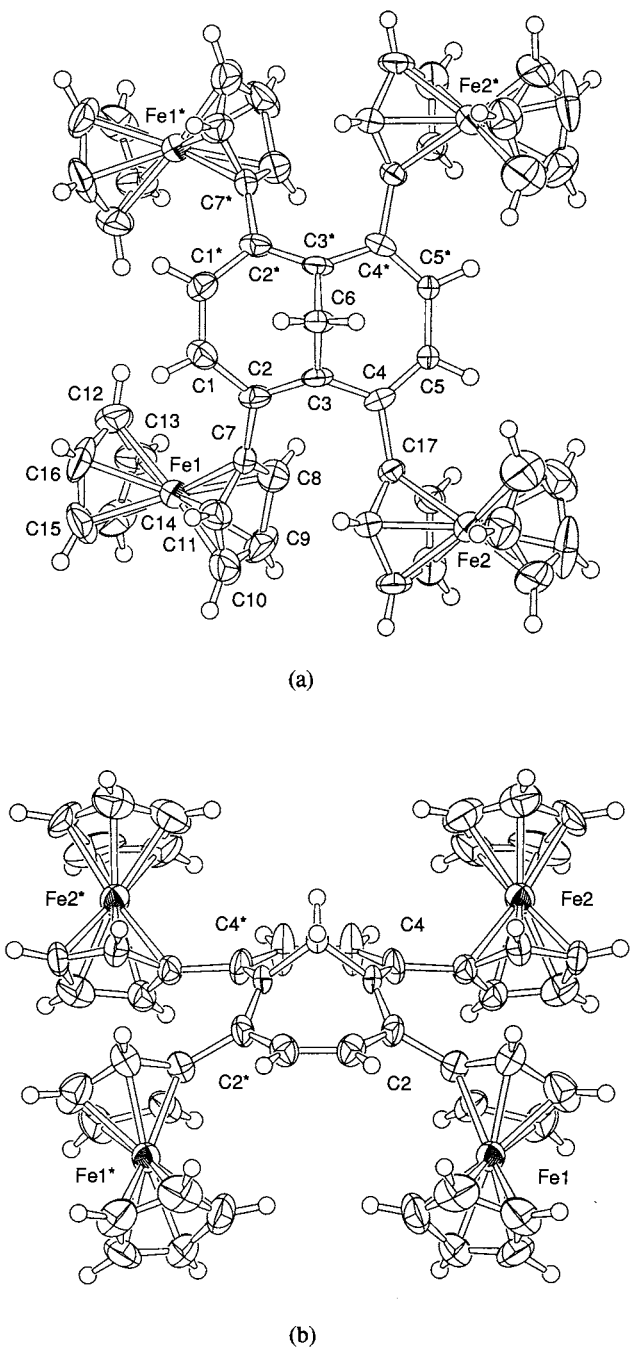

Fig. 2. The molecular structure of **9**. (a) Top view. (b) Side view.

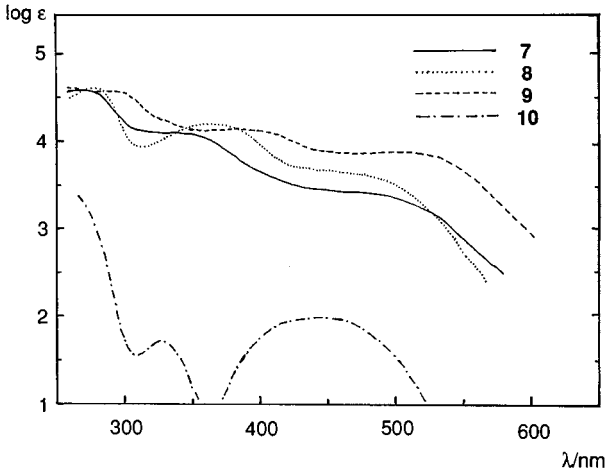

Fig. 3. The UV-vis spectra of **7**–**10** in CH_2CL_2.

enyl proton (H_b) and four multiplets of protons (H_c-H_f) attached to the annulene ring. The X-ray analyses of **7** and **9** show that the two cyclopentadienyl rings are located face-to-face. Therefore, the protons (H_c-H_f) receive a ring current effect of the faced cyclopentadienyl ring to shift to upper field, whereas the cyclopentadienyl ring is connected to the annulene ring which shifts the protons (H_e-H_f) to lower field and the proton (H_c) to upper field. The H_c-proton may be located under the annulene ring and receives its shielding effect. On the contrary, the protons (H_c-H_f) in **8** are located at the outer side of the annulene ring and hence receive its deshielding effect. Thus, the H_c-H_f protons show lower field shift at δ 4.33–5.05.

Interestingly, the chemical shifts of the methylene protons (H_a) in **7**–**9** reflect the ring strain for the annulene framework. The H_a proton in **8** shows the resonance at δ −0.15, slightly lower than the corresponding δ −0.50 in the parent 1,6-methano[10]-annulene (**16**). In contrast, the H_a protons in **7** and **9** show fairly lower shift at δ −0.04 and 0.35, respectively, presumably due to the deformation of the annulene ring which diminishes the shielding effect with smaller aromatic ring current.

The UV-vis spectra of **7**–**9** with ferrocene (**10**) show long wavelength absorptions, reflecting their orange to red colors. As shown in Fig. 3, the UV-vis spectra of **7** and **8** are similar to that of **9** but different from that of **10**. Thus, the spectra of **7** and **8** are made up of a combination of those of 1,6-methano[10]annulene and ferrocene. Since the spectrum of **9** shows a small bathochromic shift as compared with those of **7** and **8**, the four ferrocene moieties interact only a little in the excited state.

2.2.3. Redox properties

The cyclic voltammetric analysis of diferrocenyl- and tetraferrocenyl-1,6-methano[10]annulene (**7**–**9**), 1,8-diferrocenylnaphthalene (**15**), and ferrocene (**10**) are summarized in Table 5. As has been reported previously, **15** shows two one-electron oxidations ([2]a). Similarly, **7** and **8** indicate two one-electron oxidations, reflecting the interaction of the two ferrocenyl groups in **7** and **8**. Interestingly, **9** shows three oxidation potentials corresponding to two one-electron and one two-electron oxidations. As shown in Table 5, the first oxidation potentials of **7**, **9** and **15** are much lower than that of

Table 1
Crystallographic data for diffraction studies of 2,10-diferrocenyl- and 2,5,7,10-tetraferrocenyl-1,6-methano[10]annulenes (**7** and **9**)

	7	**9**
Crystal parameters		
Empirical formula	$C_{31}H_{26}Fe_2$	$C_{51}H_{42}Fe_4$
Molecular weight	M = 510.24	M = 878.28
Color	Red	Red
Crystal size (mm)	$0.35\times0.20\times0.35$	$0.15\times0.13\times0.13$
Habit	Prism	Prism
Crystal system	Monoclinic	Orthorhombic
Space group	$P2_1/a$ (No. 14)	*Pnma* (No. 62)
a (Å)	10.333(2)	7.537(7)
b (Å)	10.708(3)	25.697(6)
c (Å)	20.822(2)	20.492(3)
β (°)	91.324(10)	
V (Å^3)	$U = 2303.1(6)$	$U = 3968(3)$
Z	4	4
D_{calc} (g cm^{-3})	1.471	1.470
μ (cm^{-1})	12.76	14.67
$F(000)$	1056.00	1808.00
Intensity data		
Diffractometer	Rigaku AFC7R	Rigaku AFC7R
λ (Mo–K_a radiation)	0.71069	0.71069
Monochrometer	Graphite	Graphite
Reflections measured	$+h,+k,\pm l$	$+h,+k,-l$
2θ range (°)	<55	<55
Temperature (°C)	23	23
Scan type	$\omega-2\theta$	$\omega-2\theta$
Scan speed (deg min^{-1})	16	16
Scan width (°)	$1.73+0.35\tan\theta$	$1.78+0.35\tan\theta$
bkgd measurement	50% scan time	50% scan time
Standard reflections	3 in every 150	3 in every 150
No. of reflections collected	5912	5174
No. of reflections used	3304	1741
Acceptance criterion	$\|F\|/\sigma(\|F\|)>3.0$	$\|F\|/\sigma(\|F\|)>3.0$
Corrections	Lorentz-polarization Absorption (Psi scans) Secondary extinction	Lorentz-polarization
Structure solution		
Method	Direct/Fourier	Direct/Fourier
Programs	teXsan	teXsan
Scattering factors	[17]	[17]
R	0.036	0.070
R_w	0.026	0.060
Weighting scheme	$w=\sigma^2(F)^{-1}$	$w=\sigma^2(F)^{-1}$
H refinement	Isotropic	Calculated

Table 2
Selected bond distances (Å) and angles (°) for **7**

Bond distances (Å)			
Fe(1)–C(12)	2.057(3)	Fe(1)–C(13)	2.040(4)
Fe(1)–C(14)	2.020(4)	Fe(1)–C(15)	2.034(4)
Fe(1)–C(16)	2.022(4)	Fe(1)–C(17)	2.016(4)
Fe(1)–C(18)	2.017(4)	Fe(1)–C(19)	2.026(4)
Fe(1)–C(20)	2.032(4)	Fe(1)–C(21)	2.027(4)
Fe(2)–C(22)	2.050(3)	Fe(2)–C(23)	2.023(4)
C(1)–C(2)	1.391(4)	C(1)–C(10)	1.444(4)
C(1)–C(11)	1.484(4)	C(2)–C(3)	1.421(4)
C(2)–C(12)	1.496(4)	C(3)–C(4)	1.375(5)
C(4)–C(5)	1.395(6)	C(5)–C(6)	1.372(5)
C(6)–C(7)	1.419(5)	C(6)–C(11)	1.476(5)
C(7)–C(8)	1.349(6)	C(8)–C(9)	1.421(6)
C(9)–C(10)	1.365(4)	C(10)–C(22)	1.464(4)
C(12)–C(13)	1.418(5)	C(12)–C(16)	1.416(5)
C(13)–C(14)	1.410(5)	C(14)–C(15)	1.382(6)
C(15)–C(16)	1.404(6)	C(17)–C(18)	1.393(6)
C(17)–C(21)	1.380(6)	C(18)–C(19)	1.407(6)
C(19)–C(20)	1.383(6)	C(20)–C(21)	1.387(6)
Bond angles (°)			
C(12)–Fe(1)–C(17)	108.0(2)	C(12)–Fe(1)–C(18)	123.6(2)
C(2)–C(1)–C(10)	130.4(3)	C(2)–C(1)–C(11)	115.4(3)
C(10)–C(1)–C(11)	113.9(3)	C(1)–C(2)–C(3)	120.7(3)
C(1)–C(2)–C(12)	122.6(3)	C(3)–C(2)–C(12)	116.5(3)
C(2)–C(3)–C(4)	127.8(4)	C(5)–C(6)–C(7)	127.3(4)
C(1)–C(10)–C(22)	120.4(3)	C(9)–C(10)–C(22)	120.7(3)
C(1)–C(11)–C(6)	101.6(3)	Fe(1)–C(12)–C(2)	129.9(2)

ferrocene, whereas a similar potential of **8** is only slightly lower than that of ferrocene. The difference between **7** and **8** depends on the mode of the two ferrocenyl groups. The two ferrocenyl groups at the 2,10-position (1,3-cross conjugation) in **7** can communicate weakly via through-bond and through-space interaction. On the other hand, the two ferrocenyl groups in **8** are located at the 2,7-position (1,6-conjugation) and can interact strongly, but the interaction of the two ferrocenyl groups in **7** is stronger than that in **8**. It is worth noting that the first oxidation potential (one-electron) in **9** shows the lowest potential (-0.15), followed by the second one-electron (-0.06) and the third two electron oxidations ($+0.05$). Since the 1,4-interaction in **9** may be small based on other systems like 1,4-diferrocenylbenzene [7], the 1,3-interaction in **9** causes the biggest separation of the oxidation potentials ($\Delta E = 0.20$) in this series of compounds.

Table 3
Selected bond distances (Å) and angles (°) for **9**

Bond distances (Å)			
Fe(1)–C(7)	2.06(1)	Fe(1)–C(8)	2.06(1)
Fe(1)–C(9)	2.03(1)	Fe(1)–C(10)	2.00(1)
Fe(1)–C(11)	2.03(1)	Fe(1)–C(12)	2.06(1)
Fe(1)–C(13)	2.02(1)	Fe(1)–C(14)	2.01(1)
e(1)–C(15)	2.00(1)	Fe(1)–C(16)	2.03(1)
C(1)–C(1*)	1.39(2)	C(1)–C(2)	1.39(2)
C(2)–C(3)	1.43(2)	C(2)–C(7)	1.48(2)
C(3)–C(4)	1.43(2)	C(3)–C(6)	1.46(2)
C(4)–C(5)	1.32(2)	C(4)–C(17)	1.49(1)
C(5)–C(5*)	1.42(2)	C(7)–C(8)	1.42(2)
C(7)–C(11)	1.37(2)	C(8)–C(9)	1.43(2)
C(9)–C(10)	1.40(2)	C(10)–C(11)	1.38(2)
C(12)–C(13)	1.42(2)	C(12)–C(16)	1.36(2)
C(13)–C(14)	1.28(2)	C(14)–C(15)	1.40(2)
C(15)–C(16)	1.40(2)		
Bond angles (°)			
C(7)–Fe(1)–C(12)	110.6(5)	C(7)–Fe(1)–C(16)	117.8(6)
C(1*)–C(1)–C(2)	127.7(7)	C(1)–C(2)–C(3)	119(1)
C(1)–C(2)–C(7)	118(1)	C(3)–C(2)–C(7)	122(1)
C(2)–C(3)–C(4)	128(1)	C(2)–C(3)–C(6)	116(1)
C(3)–C(6)–C(3*)	102(1)		

2.2.4. ^{57}Fe Mössbauer spectroscopy

The oxidation potentials in Table 5 show that diferrocenyl- and tetraferrocenyl-1,6-methano[10]annulene (**7**–**9**) can be oxidized easily. Therefore, we tried the oxidation of **7** with molecular iodine. When a solution of **7** in CH_2Cl_2 was mixed with a solution of iodine (excess), the black needles of $\mathbf{7}^{2+} \cdot 2I_3^-$ were formed in 91% yield. This oxidation product was characterized by the ^{57}Fe Mössbauer spectroscopy as shown in Table 6. The spectrum of $\mathbf{7}^{2+} \cdot I_3^-$ showed more than 90% of ferrocenium signals, and a small signal of the Fe(II) species remained unchanged. Although the two ferrocenium groups in $\mathbf{7}^{2+} \cdot 2I_3^-$ may interact ferromagnetically, they are concluded to be magnetically independent above 77K (Fig. 7).

3. Experimental

3.1. General

Microanalysis were performed by the Microanalytical Service at the Department of Chemistry, Tokyo Metropolitan University. ^{1}H- and ^{13}C-NMR spectra were recorded on a JEOL JNM-EX400 or JNM-LA500 instrument, using TMS as an internal standard. Electronic spectra were obtained on a Shimazu UV-3101PC instrument and are reported in nanometers (log ε) (sh = shoulder). Mass spectral analysis (MS) were performed on a JEOL JMS-AX500 instrument, and only the more intense or structurally diagnostic mass spectral fragment ion peaks are reported. Electrochemical measurements were carried out by cyclic voltammetry using a standard three-electrode cell on a BAS CV-27 analyzer. All potentials were referenced to FcH/FcH^+, which had a potential of $+0.31$ V versus Ag/Ag^+ in this medium. Melting points were determined on a Yanaco MP-500D apparatus and are uncorrected. Column chromatography was carried out with use of Daisogel IR-60 1001W (63–210 mesh). Analytical TLC was performed by using plates of Merck silica gel 60 F_{254} and alumina 60 F_{254} TLC plates. Gel-permeation chromatography (GPC) was performed by means of a

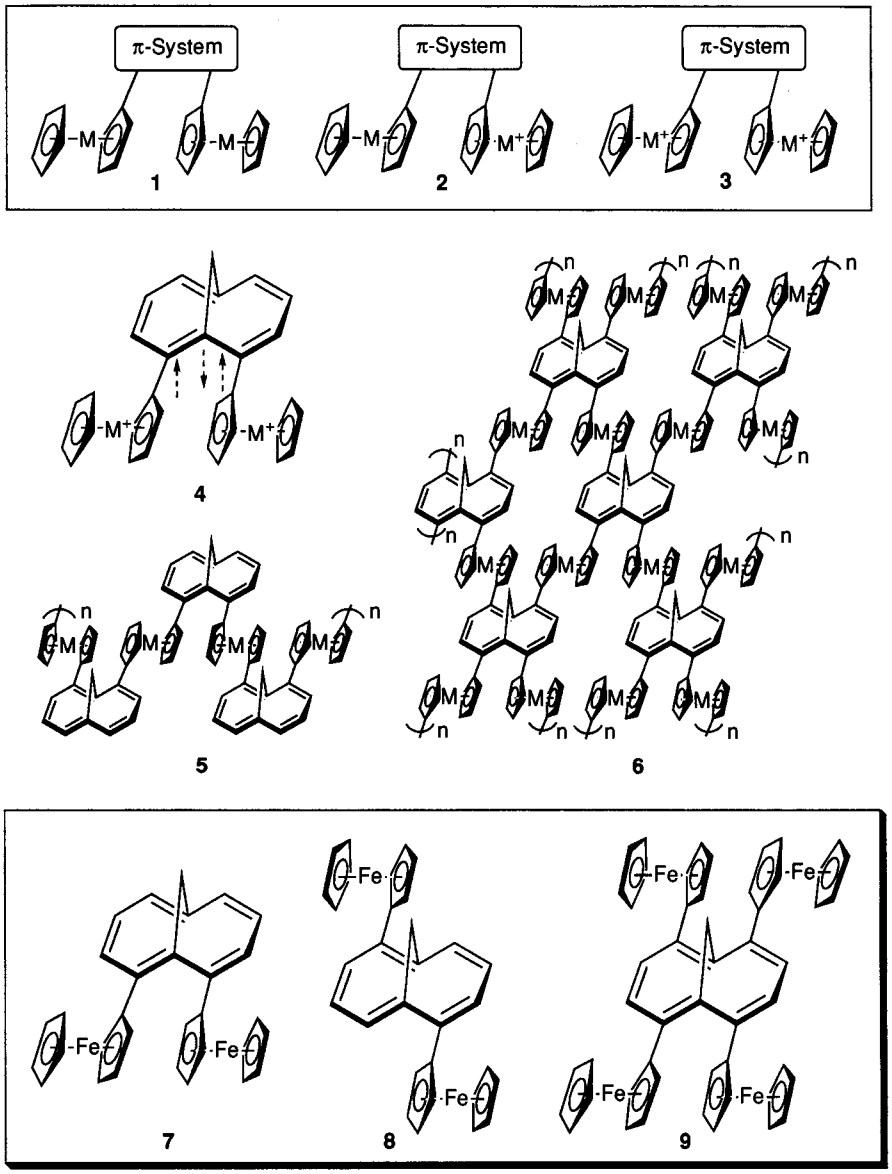

Fig. 4.

JAI model LC-908 liquid chromatography equipped with two JAIGEL-1H columns (20 × 600 mm) with chloroform as eluent.

3.2. 2,10-Diferrocenyl-1,6-methano[10]annulene (7)

To a solution of ferrocene (**10**, 558 mg, 3 mmol) in dry THF (2.5 ml) was added a 1.60 M solution of *t*-butyllithium in pentane (2.5 ml, 4 mmol) at 0°C under nitrogen atmosphere to produce a dark orange precipitate. After stirring at 0°C for 30 min, a solution of zinc chloride (454 mg, 3.22 mmol) in THF (3 ml) was added. After 15 min at 0°C, the reaction mixture was allowed to warm to room temperature and stirred for 1 h to give an orange suspension of **11**. To the resulting mixture was added a solution of 2,10-dibromo-1,6-methano[10]annulene (**12**, 301 mg, 1 mmol) in THF (3 ml), followed by the addition of a suspension of $PdCl_2(PPh_3)_2$ (71 mg, 0.1 mmol) in THF (3 ml) to form a reddish-orange solution which was changed to a dark red solution. After stirring at the same temperature for 1 h, 2M solution (3 ml) of hydrochloric acid was added, and the organic layer was separated. The water layer was extracted with THF, and the combined organic phase was washed with aq. NaCl solution and dried over $MgSO_4$. After removal of the solvent in vacuo, the reaction products were separated by column chromatography on silica gel (hexane/CH_2Cl_2 4:1) to give **7** (249 mg) in 49% yield. **7**, red crystals, m.p. 180–182°C, EI-MS *m*/*z* (relative intensity) 510 (100, M^+), 445 (8), 324 (15); ^{1}H-NMR ($CDCl_3$) δ 7.75 (d, $J = 9.8$ Hz, 2H), 7.25 (d, $J = 8.9$, 2H), 7.08 (dd, $J = 9.8$, 8.9, 2H), 4.35

Table 4
^{1}H-NMR parameters of **7**–**9** in $CDCl_3$ at room temperature

Compound	^{1}H-NMR Parameters (δ)
7	−0.04 (s, Ha), 3.78 (m, Hc), 3.86 (m, Hd or He), 3.91 (s, Hb), 3.94 (m, He or Hd, 4.35 (m, Hf), 7.08 (dd, Hh), 7.25 (d, Hi), 7.75 (d, Hg)
8	−0.15 (s, Ha), 4.20 (s, Hb), 4.33 (m, Hd or He), 4.37 (m, He or Hd), 4.42 (m, Hc), 5.05 (m, Hf), 6.98 (dd, Hh), 7.57 (d, Hi), 7.67 (d, Hg)
9	0.35 (s, Ha), 3.91 (m, Hd, He), 3.97 (m, Hc), 4.01 (s, Hb), 4.34 (m, Hf), 7.69 (s, Hg)

(m, 2H), 3.94 (m, 2H), 3.91 (s, 10H), 3.86 (m, 2H), 3.78 (m, 2H), −0.04 (s, 2H); ^{13}C-NMR ($CDCl_3$) δ 139.3, 130.9, 126.2, 125.8, 123.1, 115.0 (annulene-sp^2), 88.2, 70.2, 70.1, 69.4, 67.1, 67.0 (Cp), 37.3 (CH_2); UV-vis λ_{max} (CH_2Cl_2) 271 (log ε 4.58), 352 sh (4.08), 481 (3.42) nm. Anal. Calc. for $C_{31}H_{26}Fe_2$: C, 72.97; H, 5.14. Found: C, 72.97; H, 5.15.

3.3. 2,7-Diferrocenyl-1,6-methano[10]annulene (8)

To a solution of ferrocene (**10**, 558 mg, 3 mmol) in THF (2.5 ml) was added a 1.60 M solution of *t*-butyllithium in pentane (2.5 ml, 4 mmol) at 0°C. After 30 min, a solution of zinc chloride (454 mg, 3.22 mmol) in THF (3 ml) was added at 0°C and stirred for 15 min. The reaction mixture was allowed to warm to room temperature and stirred for 1 h. To the mixture was added a solution of 2,7-dibromo-1,6-methano[10]-annulene (**13**, 301 mg, 1 mmol) in THF (5 ml), followed by the addition of a suspension of $PdCl_2(PPh_3)_2$ (71 mg, 0.1 mmol) in THF (5 ml). After stirring at room temperature for 1 h, 2M solution (3 ml) of hydrochloric

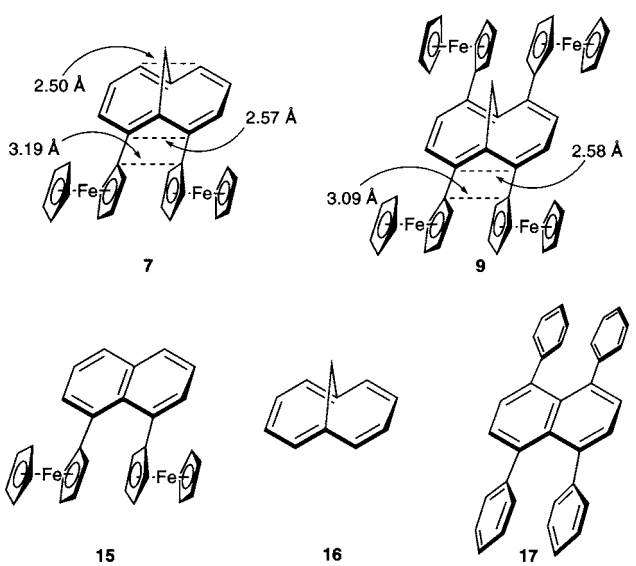

Fig. 5.

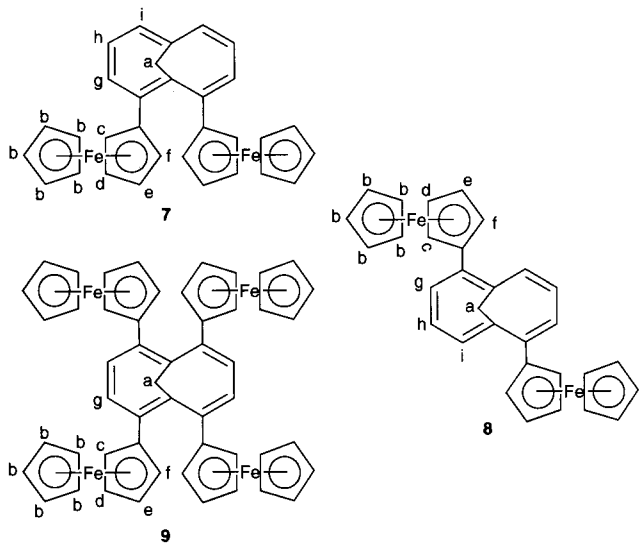

Fig. 6.

acid was added, and the organic layer was separated. The water layer was extracted with THF, and the combined organic phase was washed with aq. NaCl solution and dried over $MgSO_4$. After evaporation of the solvent, the products were separated by column chromatography on silica gel (hexane/CH_2Cl_2) to give **8** (240 mg) in 47% yield. **8**, orange crystals, m.p. 265°C (decomposition), EI-MS *m*/*z* (relative intensity) 510 (100, M^+), 324 (7); ^{1}H-NMR ($CDCl_3$) δ 7.67 (d, J = 8.8 Hz, 2H), 7.57 (d, J = 9.8, 2H), 6.98 (dd, J = 9.8, 8.8, 2H), 5.05 (m, 2H), 4.42 (m, 2H), 4.37 (m, 2H), 4.33 (m, 2H), 4.20 (s, 10H), −0.15 (s, 2H); ^{13}C-NMR ($CDCl_3$) δ 139.9, 128.4, 126.9, 126.8, 117.7 (annulene-sp^2), 85.6, 71.8, 69.8, 69.0, 68.7 (Cp), 36.4 (CH_2); UV-vis λ_{max} (CH_2Cl_2) 279 (log ε 4.61), 362 (4.19), 480 sh (3.61) nm. Anal. Calc. for $C_{31}H_{26}Fe_2$: C, 72.97; H, 5.14. Found: C, 72.66; H, 5.14.

3.4. 2,5,7,10-Tetraferrocenyl-1,6-methano[10]annulene (9)

To a solution of ferrocene (**10**, 1.12 g, 6 mmol) in THF (4 ml) was added a 1.64 M solution of *t*-butyl-

Table 5
Redox potentials of **7**–**9**, **10**, and **15** measured by cyclic voltammetry

Compound	$E^1_{1/2}$	$E^2_{1/2}$	$E^3_{1/2}$	ΔE
7	−0.11	0.03		0.14
8	−0.04	0.03		0.07
9	−0.15	−0.06	0.05	0.09, 0.11
15	−0.13	0.04		0.17
10	0			—

Conditions: V versus Fe/Fe^+, n-Bu_4NClO_4 (0.1 mol l^{-1}), benzonitrile, 20°C, Pt working and counter electrodes, Ag/Ag^+ reference electrode.

Table 6
^{57}Fe Mössbauer parameters of $\mathbf{7}^{2+}\cdot 2(I_3)^-$

T (K)	δ (mm s^{-1})	ΔE_Q (mm s^{-1})	Γ (mm s^{-1})
298	0.34	0.22	0.26
77	0.53	0.25	0.38, 0.28

lithium in pentane (4.9 ml, 8 mmol) at 0°C. After 30 min, a solution of zinc chloride (1.21 g, 8.6 mmol) in THF (10 ml) was added at 0°C and stirred for 15 min. The reaction mixture was allowed to warm to room temperature and stirred for 1 h. To the mixture was added a solution of 2,5,7,10-tetrabromo-1,6-methano-[10]annulene (**14**, 458 mg, 1 mmol) in THF (5 ml), followed by the addition of $PdCl_2(PPh_3)_2$ (141 mg, 0.2 mmol) in THF (2 ml). After stirring at room temperature for 1 h, 2M solution (5 ml) of hydrochloric acid was added, and the organic layer was separated. The water layer was extracted with THF, and the combined organic phase was washed with aq. NaCl solution and dried over $MgSO_4$. After evaporation of the solvent, the products were separated by column chromatography on silica gel (hexane/CH_2Cl_2), followed by purification by gel-permeation chromatography to afford **9** (202.5 mg) in 29% yield. **9**, red crystals, m.p. 245°C (decomposition), FAB-MS m/z 878 (M^+), 823, 692; ^{1}H-NMR ($CDCl_3$) δ 7.69 (s, 4H), 4.34 (m, 4H), 4.01 (s, 20H), 3.97 (m, 4H), 3.91 (m, 8H), 0.35 (s, 2H); ^{13}C-NMR ($CDCl_3$) δ 136.2, 130.6, 121.2 (annulene-sp^2), 88.6, 70.4, 70.3, 69.4, 67.2, 67.1 (Cp), 39.6 (CH_2); UV-vis λ_{max} (CH_2Cl_2) 291 (log ε 4.57), 383 (4.14), 407 sh (3.88) nm. Anal. Calc. for $C_{51}H_{42}Fe_4$: C, 69.75; H, 4.82. Found: C, 69.73; H, 4.75.

3.5. Oxidation of 7 with molecular iodine

To a solution of **7** (76.5 mg, 0.15 mmol) in CH_2Cl_2 (10 ml) was added a solution of I_2 (152 mg, 1.2 mmol) in CH_2Cl_2 (10 ml) under nitrogen atmosphere at room temperature. After stirring for 30 min, hexane (5 ml) was carefully added to form a black precipitate of $\mathbf{7}^{2+}\cdot 2I_3^-$ (174 mg, 91%). Anal. Calc. for $C_{31}H_{26}Fe_2I_6$: C, 29.28; H, 2.06. Found: C, 30.69; H, 2.26.

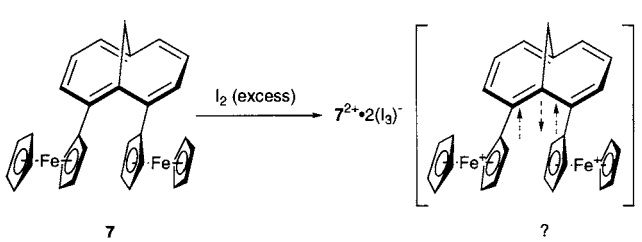

Fig. 7.

3.6. X-ray structure determinations of 7 and 9

Either prismatic crystal of **7** or **9** was mounted on a glass fiber. All measurements were made on a Rigaku AFC7R diffractmeter with graphite monochromated Mo–K_α radiation and a 12 kW rotating anode generator. The cell dimension was obtained from a least-squares refinement using the setting angles of 25° carefully centered reflections. The data were collected at a speed of 16°/min using the ω-2θ scan technique to a maximum 2θ value of 55.1°. The weak reflections ($I < 10.0\sigma(I)$) were rescanned (maximum of 5 scans) and the counts were accumulated to ensure good counting statistics. As for **7**, an empirical absorption correction based on azimuthal scans of several reflections was applied. The data were corrected for Lorentz and polarization effect, and for secondary extinction for **7**. The structure was solved by direct methods and expanded using Fourier techniques. The non-hydrogen atoms were refined anisotropically. Hydrogen atoms were refined isotropically for **7** and were included but not refined for **9**. The final cycle of full-matrix least-squares refinement was based on 3304 for **7** or 1741 for **9** observed reflections and 403 for **7** or 250 for **9** variable parameters and converged. No trend in ΔF versus F_o or sin θ/λ was observed. Final difference synthesis showed no significant electron density (no greater than 0.3 eÅ^{-3}). Neutral atom scattering factors were taken from Cromer and Waber [17]. Anomalous dispersion effects were included in F_{calc} [18]; the values for $\Delta f'$ and $\Delta f''$ were those of Creg and McAuley [19]. Most of the calculations were carried out with the teXsan system [20].

References

[1] (a) J.K. Burdett, E. Canadell, Organometallics 4 (1985) 805. (b) J.M. Manriquez, M.D. Ward, T.C. Calabrese, P.J. Fagan, A.J. Epstein, J.S. Miller, Mol. Cryst. Liq. Cryst. 176 (1989) 527.
[2] (a) M.T. Lee, B.M. Foxman, M. Rosenblum, Organometallics 4 (1985) 539. (b) R. Arnold, S.A. Matchett, M. Rosenblum, Organometallics 7 (1988) 2261. (c) D.A. Gronbeck, S.A. Matchett, M. Rosenblum, Tetrahedron Lett. 30 (1989) 2881. (d) D.A. Gronbeck, S.A. Matchett, M. Rosenblum, Tetrahedron Lett. 31 (1990) 4977.
[3] (a) I. Manners, Angew. Chem. Int. Ed. Engl. 35 (1996) 1603. (b) D. Astruc, Acc. Chem. Res. 30 (1997) 383.
[4] (a) W.H. Morrison, D.N. Hendrickson, Inorg. Chem. 14 (1975) 2331. (b) J.A. Kramer, D.N. Hendrickson, Inorg. Chem. 19 (1980) 3330. (c) F. Delgado-Pena, D.R. Talham, D.O. Cowan, J. Organomet. Chem. 253 (1983) C43.
[5] T.Y. Dong, C.K. Chang, S.H. Lee, L.L. Lai, M.Y.N. Chiang, K.J. Lin, Organometallics 16 (1997) 5816.
[6] (a) M. Iyoda, T. Okabe, T. Kondo, S. Sasaki, H. Matsuyama, Y. Kuwatani, M. Katada, Mol. Cryst. Liq. Cryst. 286 (1996) 65. (b) M. Iyoda, T. Okabe, T. Kondo, S. Sasaki, Y. Kuwatani, M. Katada, Chem. Lett. (1997) 103.

[7] M. Iyoda, T. Kondo, T. Okabe, H. Matsuyama, S. Sasaki, Y. Kuwatani, Chem. Lett. (1997) 35.
[8] (a) E. Vogel, W.A. Böll, M. Biskup, Tetrahedron Lett. (1966) 1569. (b) E. Vogel, K.D. Sturm, A. de Faries Dias, J. Lex, H. Schmickler, F. Wudl, Angew. Chem. Int. Ed. Engl. 24 (1985) 590.
[9] E. Vogel, W.A. Böll, Angew. Chem. 76 (1964) 784.
[10] W. Bornatsch, E. Vogel, Angew. Chem. 87 (1975) 412.
[11] R. Bianchi, T. Pilati, M. Simonetta, Acta Cryst. B36 (1980) 3146.
[12] P.G. Evrard, P. Piret, M. Van Meerssche, Acta Cryst. B28 (1972) 497.
[13] H.O. House, D.G. Koepsell, W.J. Campbell, J. Org. Chem. 37 (1972) 1003.
[14] R. Neidlein, W. Wirth, A. Gieren, V. Lamm, T. Hübner, Angew. Chem. Int. Ed. Engl. 24 (1985) 587.
[15] E. Vogel, H.D. Roth, Angew. Chem. 76 (1964) 145.
[16] (a) H.O. House, W.J. Campbell, M. Gall, J. Org. Chem., 35 (1970) 1815. (b) R.L. Clough, J.D. Roberts, J. Am. Chem. Soc. 98 (1976) 1018.
[17] D.T. Cromer, J.T. Waber, International Tables for X-ray Crystallography, vol. 4, Kynoch, Birmingham, 1974 Table 2.2A.
[18] J.A. Ibers, W.C. Hamilton, Acta Crystallogr. 17 (1964) 781.
[19] D.C. Cregh, W.J. McAuley, in: A.J.C. Wilson (Ed.), International Tables for Crystallography, vol. C, Kluwer Academic, Boston, 1992, pp. 219–222 Table 4.2.6.8.
[20] teXsan: Crystal Structure Analysis Package, Molecular Structure Corporation (1985 and 1992).